

Citation for published version:

Wang, C, Cui, B, Wang, Z & Gu, C 2019, 'SDP-based Optimal Power Flow with Steady-State Voltage Stability Constraints', *IEEE Transactions on Smart Grid*, vol. 10, no. 4, 8439024, pp. 4637-4647.
<https://doi.org/10.1109/TSG.2018.2866068>

DOI:

[10.1109/TSG.2018.2866068](https://doi.org/10.1109/TSG.2018.2866068)

Publication date:

2019

Document Version

Peer reviewed version

[Link to publication](#)

© 2018 IEEE. Personal use of this material is permitted. Permission from IEEE must be obtained for all other users, including reprinting/ republishing this material for advertising or promotional purposes, creating new collective works for resale or redistribution to servers or lists, or reuse of any copyrighted components of this work in other works.

University of Bath

Alternative formats

If you require this document in an alternative format, please contact:
openaccess@bath.ac.uk

General rights

Copyright and moral rights for the publications made accessible in the public portal are retained by the authors and/or other copyright owners and it is a condition of accessing publications that users recognise and abide by the legal requirements associated with these rights.

Take down policy

If you believe that this document breaches copyright please contact us providing details, and we will remove access to the work immediately and investigate your claim.

SDP-based Optimal Power Flow with Steady-State Voltage Stability Constraints

Chong Wang, *Member, IEEE*, Bai Cui, *Student Member, IEEE*, Zhaoyu Wang, *Member, IEEE* and Chenghong Gu, *Member, IEEE*

Abstract—This paper proposes a voltage stability-constrained optimal power flow (VSC-OPF) model based on semidefinite programming (SDP) relaxation. The minimum singular value of the power flow Jacobian is used as a steady-state voltage stability index, which is incorporated into the semidefinite programming formulation. To model a semidefinite programming constraint for voltage stability, an auxiliary matrix based on the power flow Jacobian is constructed, and this auxiliary matrix can be reformulated as a function of the semidefinite variable matrix defined for semidefinite programming relaxation. The resulting SDP-based VSC-OPF model is formulated and solved via the solver SDPT3 and the toolbox YALMIP. Extensive simulations on IEEE test systems validate the effectiveness of the proposed model.

Index Terms—optimal power flow, semidefinite programming, voltage stability

I. INTRODUCTION

POWER systems are undergoing stressed operation states with the increasing load demand associated with the need of economic operation. These stressed power systems are being operated ever closer to voltage stability margin [1]. In addition, more stochastic disturbances, caused by the higher penetration of renewables such as wind power and solar power [2], may jeopardize the robustness of a power system and pushing one with a low voltage stability margin to an unstable state. Usually, the security requirements, e.g., such as line flow constraints and voltage magnitude constraints in the conventional optimal power flow model, can guarantee a feasible solution in voltage stable [3]. However, a counterexample in [4] shows that the ‘nose point’ of the load PV curve may lie at a high voltage point, which means the margin to voltage instability may be small even when the system is under normal voltage levels. More generally, the system may become voltage unstable at high voltages as it gets more capacitive. Therefore, the incorporation of voltage stability constraints in OPF formulations is becoming more important.

The singularity of the power flow Jacobian matrix can be used as an indicator for steady-state stability [5]. The minimum singular value (MSV) can be used to show the distance between the steady-state voltage stability limit and the studied operating point. Based on this, Thomas and Tiranuchit [6], [7] employed the minimum singular value of

the power flow Jacobian matrix as a static voltage stability index, and the minimum singular value of the power flow Jacobian was also used for voltage collapse assessment in [8]–[10]. In addition to the minimum singular value, there are some other indices, e.g., the heuristic-based L -index [11] and the minimum eigenvalue [12], [13] for assessing the static voltage stability. Furthermore, some indices based on reduced models [14], [15] and branch-oriented models [16] have been proposed to indicate system voltage stability conditions by measurements at some critical buses. An index based on a necessary condition is developed to represent the distance between the current operating point and the power flow solvability boundary [17], [18]. The developed index only requires the present snapshots of voltage phasors to monitor the power flow insolvability and voltage stability. The above work mainly focuses on the monitoring of voltage stability. To develop ways for controlling and enhancing voltage stability, critical modes based on system modal analysis are used to identify the causes for voltage instability [19] and some remedial measures [20]–[22] are conducted to enhance voltage stability. Moreover, voltage stability has been considered in various optimization problems for either enhancing or constraining system stability levels. A voltage stability index quantifying the distance to the point of collapse is introduced for reactive power planning against voltage collapse in [23]. In [24], the problem of voltage stability enhancement by means of reactive power planning is formulated as an optimization problem, which maximizes the voltage stability margin. [25] presents a voltage stability constrained optimal power flow approach based on a voltage collapse proximity indicator (VCPI), which provides important information about the proximity of the system to voltage instability. An approximation of the Hessian matrix of the Lagrangian function is calculated at each iteration and the optimization problem is solved by using a line search procedure. [26] proposes a voltage stability-constrained optimal power flow (VSC-OPF) model based on a recently proposed sufficient condition on power flow Jacobian nonsingularity. The used condition is second-order conic representable with given load consumption. The entire model is relaxed to a second-order cone program. To apply the model to large systems, a sparse approximate approach is used. Since the minimum singular value of the power flow Jacobian is one of important static voltage stability indices, [27]–[29] incorporate the minimum singular value of the power flow Jacobian into the optimal power flow (OPF) model as a voltage stability constraint to ensure a minimum distance to the steady-state voltage stability limit. Based on the minimum singular value of the power flow Jacobian matrix and the corresponding singular vectors, [30] proposes an iteration-based method to enforce a voltage stability constraint in the optimal power flow model. Though the above papers have contributed to VSC-OPF models and solutions, however, some improvements on the model formu-

This work was partially supported by the U.S. Department of Energy Office of Electricity Delivery and Energy Reliability, the National Science Foundation under ECCS 1609080, and the Power System Engineering and Research Center (PSERC S-70). (*Corresponding author: Zhaoyu Wang.*)

Chong Wang is with the College of Energy and Electrical Engineering, Hohai University, Nanjing 211100, China (e-mail: chongwang@hhu.edu.cn).

Bai Cui is with the School of Electrical and Computer Engineering, Georgia Institute of Technology, Atlanta, GA 30332 USA (e-mail: bcui7@gatech.edu).

Zhaoyu Wang is with the Department of Electrical and Computer Engineering, Iowa State University, Ames, IA 50011, USA (email: wzy@iastate.edu).

Chenghong Gu is with the Department of Electronic and Electrical Engineering, University of Bath, Bath, BA2 7AY, UK (e-mail: C.Gu@bath.ac.uk).

lation and solution can be made to avoid the approximation of the Hessian matrix, the sparse approximation, and the iteration-based method.

SDP has been applied in various engineering problems since it is polynomially solvable and the solution is globally optimal [31], [32]. SDP relaxation of OPF problems have gained considerable attention in recent years. When one rank condition is satisfied for the relaxed model, the globally optimal solution of the original optimal power flow can be recovered [33]. Since the rank condition is not always satisfied, many research studies have been conducted to investigate scenarios under which the rank condition is satisfied. [34] shows that there is no gap for the SDP relaxation when load over-satisfaction is allowed and enough virtual phase shifters are installed. In [35], it is proven that the SDP relaxation is tight when there are no lower bounds on active and reactive power for radial networks with line flow constraints, line loss constraints and voltage magnitude constraints. Similar results are obtained in [36] and [37]. [38] shows that the SDP relaxation is tight when there are practical angle constraints and real power lower bounds for radial systems. Some papers have investigated voltage stability constrained optimal power flow by means of convex semidefinite programming. [39] develops an optimal power flow model, in which a variable representing maximum loading factor is included. The objective is to find a set of feasible operating points that ensure the maximum loading factor while minimizing the cost of increasing stability margins. For these two objectives, the weight coefficients are employed. In practice, it is difficult to set the weight coefficients. [40] introduces a maximum L-index into the optimal power flow model, and the objective is to minimize the maximum L-index. To obtain the L-index, the voltages at generator buses are assumed to be constant, but this may result in inaccurate results. The minimum singular value is an important index representing the distance between the steady-state voltage stability limit and the studied operating point, however, few studies include the constraint of the minimum singular value in the optimal power flow model due to the non-explicit and non-convex function of the minimum singular value with regard to variables in the optimization model.

To use the minimum singular value as the voltage stability and address the issue of the non-explicit and non-convex function of the minimum singular value with regard to variables, we propose an efficient way to incorporate the constraint with regard to the minimum singular value in the OPF model by formulating it as an SDP constraint. The main contributions of this paper are three-fold: 1) To achieve the explicit and convex formulation for the constraint of the voltage stability, an auxiliary matrix based on the power flow Jacobian is introduced. We then establish the equivalence between the minimum eigenvalue of the auxiliary matrix and the minimum singular value of the original power flow Jacobian. 2) The SDP relaxation of the OPF problem is used to relax the OPF problem as a convex one. The equivalent constraint on the minimum eigenvalue of the auxiliary matrix is then integrated into the convexified OPF formulation to arrive at the convex VSC-OPF formulation. 3) The proposed model is tested by using the toolbox YALMIP associate with SDPT3, and IEEE 14-bus, 30-bus, 57-bus and 118-bus systems.

The rest of the paper is organized as follows. Section II describes the conventional OPF model and its SDP relaxation. Section III presents the voltage stability constraint and its SDP reformulation, and the SDP relaxation of the VSC-OPF

model. Section IV presents extensive case studies to validate the proposed model. Concluding remarks and outline for future works are given in Section V.

II. CONVENTIONAL OPTIMAL POWER FLOW AND ITS SEMIDEFINITE PROGRAMMING RELAXATION

This section first shows the conventional OPF model, and then presents the definition of symmetric matrices and the SDP relaxation of the conventional OPF model.

A. Formulation of AC-OPF

We consider a system represented by a graph (Ω_b, Ω_l) , where $\Omega_b = \{1, 2, \dots, n\}$ is the set of all buses and Ω_l is the set of lines and transformers. For each line (transformer) $k \in \Omega_l$ has two terminal buses k_f and k_t . Define Ω_g as the set of all generators, and the $\Omega_{g,i} \subset \Omega_g$ as the set of generators connected to bus i . The general OPF formulation is shown as follows.

$$\min \sum_{g \in \Omega_g} (c_{2,g} P_{G,g}^2 + c_{1,g} P_{G,g} + c_{0,g}) \quad (1a)$$

s.t.

$$\sum_{g \in \Omega_{g,i}} P_{G,g} - P_{L,i} = \sum_{j \in \Omega_b} [V_{e,i}(V_{e,j}G_{ij} - V_{f,j}B_{ij})] + \sum_{j \in \Omega_b} [V_{f,i}(V_{f,j}G_{ij} + V_{e,j}B_{ij})] \quad i \in \Omega_b \quad (1b)$$

$$\sum_{g \in \Omega_{g,i}} Q_{G,g} - Q_{L,i} = \sum_{j \in \Omega_b} [V_{f,i}(V_{e,j}G_{ij} - V_{f,j}B_{ij})] - \sum_{j \in \Omega_b} [V_{e,i}(V_{f,j}G_{ij} + V_{e,j}B_{ij})] \quad i \in \Omega_b \quad (1c)$$

$$P_{G,g}^{\min} \leq P_{G,g} \leq P_{G,g}^{\max} \quad g \in \Omega_g \quad (1d)$$

$$Q_{G,g}^{\min} \leq Q_{G,g} \leq Q_{G,g}^{\max} \quad g \in \Omega_g \quad (1e)$$

$$(V_i^{\min})^2 \leq |V_i|^2 \leq (V_i^{\max})^2 \quad i \in \Omega_b \quad (1f)$$

$$|S_k| \leq S_k^{\max} \quad k \in \Omega_l \quad (1g)$$

where (1a) is the objective in which $c_{0,g}$, $c_{1,g}$ and $c_{2,g}$ are coefficients of the generator g . (1b)-(1g) are the operational constraints. $P_{G,g}$ and $Q_{G,g}$ are active and reactive power generation of generator g . $V_i = V_{e,i} + jV_{f,i}$ is the voltage phasor at bus $i \in \Omega_b$. $P_{G,g}^{\min}$ ($Q_{G,g}^{\min}$) and $P_{G,g}^{\max}$ ($Q_{G,g}^{\max}$) are lower and upper limits of real power (reactive power) of generator g , respectively. V_i^{\min} and V_i^{\max} are the lower and upper limits of $|V_i|$. S_k is the apparent power through line k , and S_k^{\max} is the upper limit of $|S_k|$. $P_{L,i}$ and $Q_{L,i}$ are active and reactive load of bus i . G_{ij} and B_{ij} are conductance and susceptance of line (i, j) .

B. SDP Relaxation of AC-OPF

In this section, we first introduce some symmetric matrices used for the SDP-based AC-OPF model, and then the SDP-based AC-OPF model is presented.

1) *Symmetric matrices:* We first define three matrices \mathbf{Y}_i , $\bar{\mathbf{Y}}_i$ and \mathbf{M}_i as follows.

$$\mathbf{Y}_i = \frac{1}{2} \begin{bmatrix} \text{Re}(\mathbf{y}_i + \mathbf{y}_i^T) & \text{Im}(\mathbf{y}_i^T - \mathbf{y}_i) \\ \text{Im}(\mathbf{y}_i - \mathbf{y}_i^T) & \text{Re}(\mathbf{y}_i + \mathbf{y}_i^T) \end{bmatrix} \quad (2a)$$

$$\bar{\mathbf{Y}}_i = -\frac{1}{2} \begin{bmatrix} \text{Im}(\mathbf{y}_i + \mathbf{y}_i^T) & \text{Re}(\mathbf{y}_i - \mathbf{y}_i^T) \\ \text{Re}(\mathbf{y}_i^T - \mathbf{y}_i) & \text{Im}(\mathbf{y}_i + \mathbf{y}_i^T) \end{bmatrix} \quad (2b)$$

$$\mathbf{M}_i = \begin{bmatrix} \mathbf{e}_i \mathbf{e}_i^T & 0 \\ 0 & \mathbf{e}_i \mathbf{e}_i^T \end{bmatrix} \quad (2c)$$

where \mathbf{e}_i is an i th standard basis in \mathbb{R}^n , the matrix $\mathbf{y}_i = \mathbf{e}_i \mathbf{e}_i^T \mathbf{Y}$, $\mathbf{y}_i \in \mathbb{C}^{n \times n}$ is a matrix with all zeros except that the elements in the i th are equal to those in the i th row of \mathbf{Y} , and $\mathbf{Y} \in \mathbb{C}^{n \times n}$ is the system admittance matrix, the superscript T denotes the transpose operator, $\text{Re}(\mathbf{A})$ and $\text{Im}(\mathbf{A})$ denote the real and imaginary parts of a matrix \mathbf{A} .

For a transformer k with series admittance $G_k + jB_k$ and shunt capacitance b_k , it can be equivalently represented by a Π circuit of a line in series with an ideal transformer which has a turns ratio $1 : \eta_k e^{j\alpha_k}$. Fig. 1 shows the Π circuit model with an ideal transformer. A line has the similar model with $\eta_k = 1$ and $\alpha_k = 0$. To calculate active/reactive power through lines and transformers, the following matrices are established.

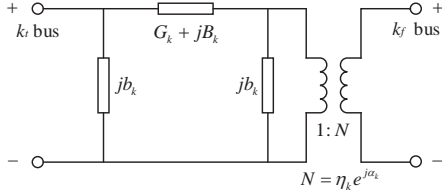


Fig. 1. Branch model.

$$\begin{aligned} \mathbf{H}_{k_f} = & \frac{G_k}{\eta_k} (\mathbf{h}_{k_f} \mathbf{h}_{k_f}^T + \mathbf{h}_{k_f+n} \mathbf{h}_{k_f+n}^T) \\ & - a_{k_f} (\mathbf{h}_{k_f} \mathbf{h}_{k_t}^T + \mathbf{h}_{k_t} \mathbf{h}_{k_f}^T + \mathbf{h}_{k_f+n} \mathbf{h}_{k_t+n}^T + \mathbf{h}_{k_t+n} \mathbf{h}_{k_f+n}^T) \\ & + b_{k_f} (\mathbf{h}_{k_f} \mathbf{h}_{k_t+n}^T + \mathbf{h}_{k_t+n} \mathbf{h}_{k_f}^T - \mathbf{h}_{k_f+n} \mathbf{h}_{k_t}^T - \mathbf{h}_{k_t} \mathbf{h}_{k_f+n}^T) \end{aligned} \quad (3a)$$

$$\begin{aligned} \mathbf{H}_{k_t} = & G_k (\mathbf{h}_{k_t} \mathbf{h}_{k_t}^T + \mathbf{h}_{k_t+n} \mathbf{h}_{k_t+n}^T) \\ & - a_{k_t} (\mathbf{h}_{k_f} \mathbf{h}_{k_t}^T + \mathbf{h}_{k_t} \mathbf{h}_{k_f}^T + \mathbf{h}_{k_f+n} \mathbf{h}_{k_t+n}^T + \mathbf{h}_{k_t+n} \mathbf{h}_{k_f+n}^T) \\ & + b_{k_t} (\mathbf{h}_{k_f+n} \mathbf{h}_{k_t}^T + \mathbf{h}_{k_t} \mathbf{h}_{k_f+n}^T - \mathbf{h}_{k_f} \mathbf{h}_{k_t+n}^T - \mathbf{h}_{k_t+n} \mathbf{h}_{k_f}^T) \end{aligned} \quad (3b)$$

$$\begin{aligned} \bar{\mathbf{H}}_{k_f} = & - \left(\frac{B_k + b_k}{\eta_k^2} \right) (\mathbf{h}_{k_f} \mathbf{h}_{k_f}^T + \mathbf{h}_{k_f+n} \mathbf{h}_{k_f+n}^T) \\ & + a_{k_f} (\mathbf{h}_{k_f} \mathbf{h}_{k_t+n}^T + \mathbf{h}_{k_t+n} \mathbf{h}_{k_f}^T - \mathbf{h}_{k_f+n} \mathbf{h}_{k_t}^T - \mathbf{h}_{k_t} \mathbf{h}_{k_f+n}^T) \\ & + b_{k_f} (\mathbf{h}_{k_f} \mathbf{h}_{k_t}^T + \mathbf{h}_{k_t} \mathbf{h}_{k_f}^T + \mathbf{h}_{k_f+n} \mathbf{h}_{k_t+n}^T + \mathbf{h}_{k_t+n} \mathbf{h}_{k_f+n}^T) \end{aligned} \quad (3c)$$

$$\begin{aligned} \bar{\mathbf{H}}_{k_t} = & - (B_k + b_k) (\mathbf{h}_{k_t} \mathbf{h}_{k_t}^T + \mathbf{h}_{k_t+n} \mathbf{h}_{k_t+n}^T) \\ & + a_{k_t} (\mathbf{h}_{k_f+n} \mathbf{h}_{k_t}^T + \mathbf{h}_{k_t} \mathbf{h}_{k_f+n}^T - \mathbf{h}_{k_f} \mathbf{h}_{k_t+n}^T - \mathbf{h}_{k_t+n} \mathbf{h}_{k_f}^T) \\ & + b_{k_t} (\mathbf{h}_{k_f} \mathbf{h}_{k_t}^T + \mathbf{h}_{k_t} \mathbf{h}_{k_f}^T + \mathbf{h}_{k_f+n} \mathbf{h}_{k_t+n}^T + \mathbf{h}_{k_t+n} \mathbf{h}_{k_f+n}^T) \end{aligned} \quad (3d)$$

where k_f and k_t denote the two buses of the line k , \mathbf{h}_i is a i th standard basis vector in \mathbb{R}^{2n} . a_{k_f} , b_{k_f} , a_{k_t} and b_{k_t} are

expressed as

$$a_{k_f} = (G_k \cos(\alpha_k) + B_k \cos(\alpha_k + \pi/2)) / (2\eta_k) \quad (4a)$$

$$b_{k_f} = (G_k \sin(\alpha_k) + B_k \sin(\alpha_k + \pi/2)) / (2\eta_k) \quad (4b)$$

$$a_{k_t} = (G_k \cos(\alpha_k) + B_k \cos(-\alpha_k + \pi/2)) / (2\eta_k) \quad (4c)$$

$$b_{k_t} = (-G_k \sin(\alpha_k) + B_k \sin(-\alpha_k + \pi/2)) / (2\eta_k) \quad (4d)$$

We collect bus voltage phasors with their real and imaginary parts as a matrix \mathbf{X} and define a new symmetric matrix \mathbf{W} .

$$\mathbf{X} = [\text{Re}(\mathbf{V}^T), \text{Im}(\mathbf{V}^T)]^T \quad (5a)$$

$$\mathbf{W} = \mathbf{X} \mathbf{X}^T \quad (5b)$$

where $\mathbf{V} \in \mathbb{C}^n$ is the bus voltage vector, and \mathbf{X} is a variable vector in \mathbb{R}^{2n} .

With the above definition, the active/reactive power at each bus, bus voltage at each bus, and the active/reactive power flow through each line can be expressed as

$$P_i = \text{Tr}\{\mathbf{Y}_i \mathbf{W}\}, i \in \Omega_b \quad (6a)$$

$$Q_i = \text{Tr}\{\bar{\mathbf{Y}}_i \mathbf{W}\}, i \in \Omega_b \quad (6b)$$

$$|V_i|^2 = \text{Tr}\{\mathbf{M}_i \mathbf{W}\}, i \in \Omega_b \quad (6c)$$

$$P_k^{(ft)} = \text{Tr}\{\mathbf{H}_{k_f} \mathbf{W}\}, k \in \Omega_l \quad (6d)$$

$$Q_k^{(ft)} = \text{Tr}\{\bar{\mathbf{H}}_{k_f} \mathbf{W}\}, k \in \Omega_l \quad (6e)$$

$$P_k^{(tf)} = \text{Tr}\{\mathbf{H}_{k_t} \mathbf{W}\}, k \in \Omega_l \quad (6f)$$

$$Q_k^{(tf)} = \text{Tr}\{\bar{\mathbf{H}}_{k_t} \mathbf{W}\}, k \in \Omega_l \quad (6g)$$

where P_i , Q_i and V_i are active power injection, reactive power injection and bus voltage magnitude at bus i , $P_k^{(ft)}$ and $Q_k^{(ft)}$ are the active and reactive power of line k from the ‘from bus’ to the ‘to bus’, $P_k^{(tf)}$ and $Q_k^{(tf)}$ are the active and reactive power of line k from the ‘to bus’ to the ‘from bus’.

2) *SDP relaxation of AC-OPF:* With the preceding preliminaries and formulations, the SDP relaxation of the conventional AC-OPF model can be expressed as

$$\min \sum_{g \in \Omega_g} \gamma_g \quad (7a)$$

s.t.

$$\begin{bmatrix} c_{1,g} P_{G,g} + c_{0,g} - \gamma_g & \sqrt{c_{2,g}} P_{G,g} \\ \sqrt{c_{2,g}} P_{G,g} & -1 \end{bmatrix} \preceq 0 \quad g \in \Omega_g \quad (7b)$$

$$\sum_{g \in \Omega_{g,i}} P_{G,g} - P_{L,i} = \text{Tr}\{\mathbf{Y}_i \mathbf{W}\} \quad i \in \Omega_b \quad (7c)$$

$$\sum_{g \in \Omega_{g,i}} Q_{G,g} - Q_{L,i} = \text{Tr}\{\bar{\mathbf{Y}}_i \mathbf{W}\} \quad i \in \Omega_b \quad (7d)$$

$$P_{G,g}^{\min} \leq P_{G,g} \leq P_{G,g}^{\max} \quad g \in \Omega_g \quad (7e)$$

$$Q_{G,g}^{\min} \leq Q_{G,g} \leq Q_{G,g}^{\max} \quad g \in \Omega_g \quad (7f)$$

$$(V_i^{\min})^2 \leq \text{Tr}\{\mathbf{M}_i \mathbf{W}\} \leq (V_i^{\max})^2 \quad i \in \Omega_b \quad (7g)$$

$$\begin{bmatrix} -(S_k^{\max})^2 & \text{Tr}\{\mathbf{H}_{k_f} \mathbf{W}\} & \text{Tr}\{\bar{\mathbf{H}}_{k_f} \mathbf{W}\} \\ \text{Tr}\{\mathbf{H}_{k_f} \mathbf{W}\} & -1 & 0 \\ \text{Tr}\{\bar{\mathbf{H}}_{k_f} \mathbf{W}\} & 0 & -1 \end{bmatrix} \preceq 0 \quad k \in \Omega_l \quad (7h)$$

$$\begin{bmatrix} -(S_k^{\max})^2 & \text{Tr}\{\mathbf{H}_{k_t}\mathbf{W}\} & \text{Tr}\{\bar{\mathbf{H}}_{k_t}\mathbf{W}\} \\ \text{Tr}\{\mathbf{H}_{k_t}\mathbf{W}\} & -1 & 0 \\ \text{Tr}\{\bar{\mathbf{H}}_{k_t}\mathbf{W}\} & 0 & -1 \end{bmatrix} \preceq 0 \quad k \in \Omega_l \quad (7i)$$

$$\mathbf{W} \succeq 0 \quad (7j)$$

where the objective in the conventional OPF model is converted to the objective (7a) and the SDP constraint (7b). (7c) and (7d) are the real and reactive power balance constraints. (7e) is the lower and upper limits of active power for each generator. (7f) is the lower and upper limits of reactive power for each generator. (7g) is the voltage limit constraint. Considering different apparent power flow at the two buses of line k , the apparent power flow limits are equivalent to two SDP constraints (7h) and (7i). (7j) is the semidefinite relaxation constraint of the constraint (5b), and $\succeq 0$ denotes the corresponding matrix is positive semidefinite.

III. SDP-BASED VSC-OPF MODEL

SDP reformulation of the constraint on the minimum singular value of the power flow Jacobian is first given in this section, which is then incorporated in the SDP relaxation of the OPF model introduced in the last section to form the convex VSC-OPF model.

A. Convex Reformulation of Voltage Stability Constraint

The minimum singular value of the power flow Jacobian can be considered as a voltage stability index [29], representing the distance between the steady-state voltage stability limit and the studied operation point. In practice, the system operators may wish to ensure certain margin to voltage instability while maintaining a low generation cost. To this end, the problem can be represented as optimal power flow with the objective of minimizing the generation cost subject to the conventional operation constraints and the voltage stability constraint. The voltage stability constraint can be expressed as follows.

$$\sigma_{\min} \geq \sigma_c \quad (8)$$

where σ_c is the voltage stability critical index, and σ_{\min} is the minimum singular value of Jacobian. When the constraint (8) is not included in the optimal power flow model, we can obtain an operating point associated with a threshold value σ_1 for the minimum singular value representing the distance between the steady-state voltage stability limit and the studied operation point. When σ_1 is close to 0, it indicates that the system has a operating condition with low voltage stability. In this case, the voltage stability can be included to improve voltage stability. We define an index $\lambda = 100\%(\sigma_c - \sigma_1)/\sigma_1$ that represents the percentage of increase in the value of the voltage stability critical index σ_c with respect to σ_1 . The system operators could set this percentage, and a higher percentage will result in a more stable operating condition. This value can be obtained from historical data or offline simulations of plausible contingency scenarios. The specific value of the percentage depends on the requirements of the system operators.

The minimum singular value used in the paper is associated with the static power flow Jacobian which does not take system dynamics into account. Augmented models and their associated Jacobians which reflect system dynamical behaviors can be considered. It is true that the static model we use seems

to be an oversimplification since voltage stability is a dynamic phenomenon that involve electromechanical transients at both generator and load side, to say the least. However, we believe the adoption of static models for voltage stability analysis can be well justified since:

- 1 The determination of bifurcation point is irrelevant of the system dynamics [41].
- 2 The stability boundary of the differential-algebraic equation (DAE) system containing generator dynamics can be identified through the static power flow equations [42].
- 3 The time scale of the voltage stability phenomenon we are dealing with in the paper is long enough such that it is essentially a system loadability problem, for which a static model serves as a good approximation [43, Chap. 7].

Since (8) is a non-explicit and non-convex constraint with regard to variables, it is necessary to address the issue caused by the non-explicit and non-convex function of the minimum singular value so that the optimization model can be solved. To this end, we first construct an explicit expression of the power flow Jacobian using matrices defined in Section II-B1. In transmission systems, generator buses except the slack bus are usually considered as PV buses, so not only PQ buses but also PV buses are included in the the power flow Jacobian. The power flow Jacobian is composed of $\partial P_i/\partial \mathbf{X}$ and $\partial Q_i/\partial \mathbf{X}$ for PQ buses, and $\partial P_i/\partial \mathbf{X}$ and $\partial |V_i|^2/\partial \mathbf{X}$ for PV buses where

$$\frac{\partial P_i}{\partial \mathbf{X}} = \frac{\partial \text{Tr}\{\mathbf{Y}_i \mathbf{W}\}}{\partial \mathbf{X}} = \mathbf{X}^T(\mathbf{Y}_i + \mathbf{Y}_i^T) \quad i \in \Omega_{b_{pq}} \cup \Omega_{b_{pv}} \quad (9)$$

$$\frac{\partial Q_i}{\partial \mathbf{X}} = \frac{\partial \text{Tr}\{\bar{\mathbf{Y}}_i \mathbf{W}\}}{\partial \mathbf{X}} = \mathbf{X}^T(\bar{\mathbf{Y}}_i + \bar{\mathbf{Y}}_i^T) \quad i \in \Omega_{b_{pq}} \quad (10)$$

$$\frac{\partial |V_i|^2}{\partial \mathbf{X}} = \frac{\partial \text{Tr}\{\mathbf{M}_i \mathbf{W}\}}{\partial \mathbf{X}} = \mathbf{X}^T(\mathbf{M}_i + \mathbf{M}_i^T) \quad i \in \Omega_{b_{pv}} \quad (11)$$

where $\Omega_{b_{pq}}$ is the set of PQ buses, and $\Omega_{b_{pv}}$ is the set of PV buses. $\partial P_i/\partial \mathbf{X}$, $\partial Q_i/\partial \mathbf{X}$ and $\partial |V_i|^2/\partial \mathbf{X}$ are $1 \times 2n$ vectors representing the partial derivative of P_i , Q_i and $|V_i|^2$ with regard to the real/imaginary parts of bus voltages, respectively. Based on (9), (10) and (11), the power flow Jacobian can be established as follows

$$\mathbf{J} = \sum_{i=1}^n \mathbf{H}^T \mathbf{h}_i \mathbf{X}^T (\mathbf{Y}_i + \mathbf{Y}_i^T) \mathbf{H} + \sum_{i=n+1}^{2n} \mathbf{H}^T (\mathbf{I} - \mathbf{H}_{pv}) \mathbf{h}_i \mathbf{X}^T (\bar{\mathbf{Y}}_{i-n} + \bar{\mathbf{Y}}_{i-n}^T) \mathbf{H} + \sum_{i=n+1}^{2n} \mathbf{H}^T \mathbf{H}_{pv} \mathbf{h}_i \mathbf{X}^T (\mathbf{M}_{i-n} + \mathbf{M}_{i-n}^T) \mathbf{H} \quad (12)$$

where the first term on the right side of (12) constructs the partial derivative of real power with regard to the real/imaginary parts of PQ bus voltages in the Jacobian matrix, the second term represents the partial derivative of reactive power with regard to the real/imaginary parts of PQ bus voltages in the Jacobian matrix, and the third term is the partial derivative of voltage square with regard to the real/imaginary parts of PV bus voltages. \mathbf{I} is an identity matrix with the appropriate dimension, $\mathbf{H} \in \mathbb{R}^{2n \times (2n-2)}$ is defined as

$$\mathbf{H} = [\mathbf{h}_1, \dots, \mathbf{h}_{i-1}, \mathbf{h}_{i+1}, \dots, \mathbf{h}_{n+i-1}, \mathbf{h}_{n+i+1}, \dots, \mathbf{h}_n], i \in \Omega_{b_s} \quad (13)$$

where the Ω_{b_s} is the set of the slack bus. In the matrix \mathbf{H} , the standard basis vectors \mathbf{h}_i and \mathbf{h}_{n+i} , $i \in \Omega_{b_s}$ corresponding

to the slack bus are not included. By multiplying \mathbf{H}^T and \mathbf{H} , the row and the column corresponding to the reference bus are removed from the Jacobian matrix. In addition, the matrix $\mathbf{H}_{pv} \in \mathbb{R}^{2n \times 2n}$ is defined as

$$\mathbf{H}_{pv} = [\mathbf{0}, \mathbf{0}, \dots, \mathbf{h}_{i+n}, \dots, \mathbf{0}] \quad i \in \Omega_{b_{pv}} \quad (14)$$

where the standard basis $\mathbf{h}_{i+n}, i \in \Omega_{b_{pv}}$ corresponding to a PV bus is the $(i+n)$ th column in \mathbf{H}_{pv} . In (12), multiplying the matrix $\mathbf{I} - \mathbf{H}_{pv}$ in the second term of the right hand of the equation ensures that the partial derivatives of active and reactive power for PQ buses are included in the Jacobian matrix, and multiplying the matrix \mathbf{H}_{pv} in the third term of the right hand of the equation ensures that the partial derivatives of active power and the voltage magnitude square for PV buses are included in the matrix.

Based on the Jacobian matrix, we introduce an auxiliary matrix that is constructed as follows.

$$\mathbf{U} = \mathbf{J}\mathbf{J}^T \quad (15)$$

where \mathbf{U} is a $(2n-2) \times (2n-2)$ symmetric positive semidefinite matrix because it satisfies

$$\mathbf{x}^T \mathbf{U} \mathbf{x} = \mathbf{x}^T \mathbf{J} \mathbf{J}^T \mathbf{x} = \mathbf{x}^T \mathbf{J} (\mathbf{x}^T \mathbf{J})^T \geq 0, \forall \mathbf{x} \in \mathbb{R}^{2n-2} \quad (16)$$

$$\mathbf{U}^T = (\mathbf{J}\mathbf{J}^T)^T = \mathbf{J}\mathbf{J}^T = \mathbf{U} \quad (17)$$

Since \mathbf{U} is a symmetric positive semidefinite matrix, we have $\mathbf{U} = \mathbf{K}\mathbf{A}\mathbf{K}^T$ where $\mathbf{K}\mathbf{K}^T = \mathbf{I}$ and \mathbf{A} is the diagonal matrix with eigenvalues as entries. For the Jacobian matrix \mathbf{J} , we have $\mathbf{J} = \mathbf{L}\mathbf{\Xi}\mathbf{R}^T$ based on singular decomposition where \mathbf{L}, \mathbf{R} are unitary matrices (i.e., $\mathbf{L}\mathbf{L}^T = \mathbf{I}$ and $\mathbf{R}\mathbf{R}^T = \mathbf{I}$) and $\mathbf{\Xi}$ is a diagonal matrix with singular values as entries, and in consequence we have $\mathbf{J}\mathbf{J}^T = \mathbf{L}\mathbf{\Xi}\mathbf{R}^T(\mathbf{L}\mathbf{\Xi}\mathbf{R}^T)^T = \mathbf{L}\mathbf{\Xi}\mathbf{R}^T\mathbf{R}\mathbf{\Xi}^T\mathbf{L}^T = \mathbf{L}\mathbf{\Xi}\mathbf{\Xi}^T\mathbf{L}^T$. Because $\mathbf{U} = \mathbf{J}\mathbf{J}^T$ holds, we have $\mathbf{L} = \mathbf{K}$ and $\mathbf{A} = \mathbf{\Xi}\mathbf{\Xi}^T$. With the relation $\mathbf{A} = \mathbf{\Xi}\mathbf{\Xi}^T$, we have $\lambda_{\min} = \sigma_{\min}^2$. Therefore, the voltage stability constraint $\sigma_{\min} \geq \sigma_c$ can be expressed as $\lambda_{\min} \geq \sigma_c^2$ considering the positive values of σ_c and σ_{\min} .

Assume that the eigenvalues of the symmetric positive semidefinite matrix \mathbf{U} are $\lambda_1, \dots, \lambda_{2n-3}, \lambda_{\min}$, and $\lambda_1 \geq \dots \geq \lambda_{2n-3} \geq \lambda_{\min}$. We construct a matrix as listed in (18).

$$\mathbf{A} - \sigma_c^2 \mathbf{I} = \begin{bmatrix} \lambda_1 - \sigma_c^2 & & & \\ & \ddots & & \\ & & \lambda_{2n-3} - \sigma_c^2 & \\ & & & \lambda_{\min} - \sigma_c^2 \end{bmatrix} \quad (18)$$

where $\lambda_{\min} \geq \sigma_c^2$ is a necessary and sufficient condition for $\mathbf{A} - \sigma_c^2 \mathbf{I} \succeq 0$. Multiplying $\mathbf{A} - \sigma_c^2 \mathbf{I} \succeq 0$ from the left by \mathbf{K} and the right by \mathbf{K}^T results in $\mathbf{K}\mathbf{A}\mathbf{K}^T - \mathbf{K}(\sigma_c^2 \mathbf{I})\mathbf{K}^T = \mathbf{U} - \sigma_c^2 \mathbf{I} \succeq 0$.

Therefore, the minimum singular value constraint of the power flow Jacobian can be equivalently rewritten as a linear matrix inequality (LMI) constraint (19).

$$\mathbf{U} - \sigma_c^2 \mathbf{I} \succeq 0 \quad (19)$$

To obtain an explicit function of \mathbf{U} with regard to variables, we rewrite \mathbf{J} in (12) as follows.

$$\mathbf{J} = \sum_{j=1}^{2n} x_j \mathbf{A}_j, \quad \mathbf{A}_j \in \mathbb{R}^{(2n-2) \times (2n-2)} \quad (20)$$

where

$$\begin{aligned} \mathbf{A}_j = & \sum_{i=1}^n \mathbf{H}^T \mathbf{h}_i \mathbf{h}_j^T (\mathbf{Y}_i + \mathbf{Y}_i^T) \mathbf{H} + \\ & \sum_{i=n+1}^{2n} \mathbf{H}^T (\mathbf{I} - \mathbf{H}_{pv}) \mathbf{h}_i \mathbf{h}_j^T (\bar{\mathbf{Y}}_{i-n} + \bar{\mathbf{Y}}_{i-n}^T) \mathbf{H} + \\ & \sum_{i=n+1}^{2n} \mathbf{H}^T \mathbf{H}_{pv} \mathbf{h}_i \mathbf{h}_j^T (\mathbf{M}_{i-n} + \mathbf{M}_{i-n}^T) \mathbf{H} \end{aligned} \quad (21)$$

and x_j is the j th element in the vector \mathbf{X} . For a given system, the matrices $\mathbf{A}_j, j \in \{1, 2, \dots, 2n\}$ are fixed and only determined by the system topology. They can be calculated offline provided that the system topology stays the same.

With the reformulation of \mathbf{J} , the matrix \mathbf{U} can be rewritten as

$$\begin{aligned} \mathbf{U} &= \mathbf{J}\mathbf{J}^T \\ &= \left(\sum_{l=1}^{2n} x_l \mathbf{A}_l \right) \left(\sum_{j=1}^{2n} x_j \mathbf{A}_j \right) \\ &= \sum_{l=1}^{2n} \sum_{j=1}^{2n} x_l x_j \mathbf{A}_l \mathbf{A}_j = \sum_{l=1}^{2n} \sum_{j=1}^{2n} W_{lj} \mathbf{A}_l \mathbf{A}_j \end{aligned} \quad (22)$$

where W_{lj} is the element corresponding to the l th row and the j th column in the symmetric matrix \mathbf{W} . Therefore, the convex voltage stability constraint can be rewritten as

$$\sum_{l=1}^{2n} \sum_{j=1}^{2n} W_{lj} \mathbf{A}_l \mathbf{A}_j - \sigma_c^2 \mathbf{I} \succeq 0 \quad (23)$$

B. SDP-based VSC-OPF Model

With the LMI constraint on voltage stability and SDP relaxation of the conventional AC-OPF model, the VSC-OPF problem can be formulated as a SDP problem as follows.

$$\begin{aligned} \text{Objective} & \quad (7a) \\ \text{Constraints} & \quad (7b) - (7j) \\ & \quad (23) \end{aligned}$$

where the matrices $\mathbf{Y}_i, \bar{\mathbf{Y}}_i, \mathbf{M}_i, \mathbf{H}_{kf}, \bar{\mathbf{H}}_{kf}, \mathbf{H}_{kt}, \bar{\mathbf{H}}_{kt}, \bar{\mathbf{H}}_{pv}, \mathbf{A}_j$, and \mathbf{A}_l in (7b)-(7j) and (23) are calculated based on (2a)-(5b), (13) and (14), respectively.

IV. CASE STUDIES

Extensive case studies on standard IEEE instances from [44] are performed and the results are presented in this section. First of all, the proposed SDP formulation is validated, and then the effects of the voltage stability constraints on OPF problems are analyzed. The proposed algorithm has been implemented by using the toolbox YALMIP [45] and the solver SDPT3 [46]. The program is written in MATLAB. All simulations are performed on a 64-bit computer with 3.5 GHz Intel Xeon processor and 16 GB RAM.

A. Validation of the Proposed Model

This section first validates the proposed model based on SDP by testing IEEE 14-bus, 30-bus, 57-bus and 118-bus systems. We compare the results based on the proposed model with those from the iterative VSC-OPF model in [30]. The iterative VSC-OPF model is solved by the nonlinear interior point solver IPOPT in the software GAMS. Since the iterative VSC-OPF model requires that σ_c be around σ_1 , we have the benchmark test with a small increase in the stability index.

Because the iterative VSC-OPF method is based on AC-OPF and no relaxation is used, the results based on this method can be considered as the benchmark results with high accuracy. If the results based on the proposed method are close to the benchmark results, we can say that the proposed method has a good performance. For the sake of exposition, we assume that the lower and upper limits of voltage at each bus are 0.9 and 1.1. The coefficients $c_{2,g}$, $c_{1,g}$, $c_{0,g}$ for each generator are 0.01, 10, and 0, respectively. The system data can be found in [47].

Table I, Table II, and Table III show the comparison results from the proposed SDP-based VSC-OPF model and the iterative VSC-OPF model for the IEEE 14-bus system, the IEEE 30-bus system, and the IEEE 57-bus system. Table IV shows the corresponding objective values, i.e., the generation costs. It is observed that the results based on the proposed VSC-OPF model are close to the benchmark results based on the iterative VSC-OPF method.

TABLE I
COMPARISON RESULTS OF IEEE 14-BUS SYSTEM WITH $\lambda = 0.48\%$

Generator No.	Bus No.	Real Power (p.u.)		Reactive Power (p.u.)	
		IPOPT	SDP	IPOPT	SDP
1	1	0.5228	0.5229	-0.0536	-0.0465
2	2	0.5782	0.5781	0.1429	0.1484
3	3	0.7322	0.7321	0.2401	0.2405
4	6	0.6038	0.6026	0.2171	0.2005
5	8	0.6918	0.6930	0.2426	0.2482

TABLE II
COMPARISON RESULTS OF IEEE 30-BUS SYSTEM WITH $\lambda = 0.85\%$

Generator No.	Bus No.	Real Power (p.u.)		Reactive Power (p.u.)	
		IPOPT	SDP	IPOPT	SDP
1	1	0.2875	0.2889	-0.0897	-0.0772
2	2	0.3229	0.3234	0.1763	0.1579
3	3	0.3563	0.3561	0.3355	0.4468
4	6	0.3667	0.3662	0.3133	0.3153
5	8	0.2577	0.2572	0.0758	0.0773
6	8	0.3189	0.3182	0.1775	0.1797

TABLE III
COMPARISON RESULTS OF IEEE 57-BUS SYSTEM WITH $\lambda = 1.07\%$

Generator No.	Bus No.	Real Power (p.u.)		Reactive Power (p.u.)	
		IPOPT	SDP	IPOPT	SDP
1	1	2.3324	2.3367	0.2610	0.2543
2	2	1.0000	1.0000	0.5000	0.5000
3	3	1.4000	1.4000	0.5537	0.5692
4	6	1.0000	1.0000	0.1083	0.1007
5	8	2.7788	2.7747	0.6967	0.6783
6	8	1.0000	1.0000	0.0900	0.0900
7	8	3.1598	3.1596	0.6129	0.6309

For the SDP-based model, the solution is exact when the rank-one condition of the matrix \mathbf{W} is satisfied. However, the rank condition is usually not satisfied due to the relaxation. Since the matrix's rank, which is the number of the nonzero singular values, provides the information about the accuracy of the solution, Fig. 2 (a) shows the singular values of the matrix

TABLE IV
OBJECTIVE RESULT COMPARISON

Test Systems	Objective(\$/h)	
	IPOPT	SDP
IEEE 14	3327.39	3327.38
IEEE 30	1971.58	1971.56
IEEE 57	15481.47	15481.29
IEEE 118	54235.40	54167.86

\mathbf{W} for the IEEE 14-bus system with different thresholds of the voltage stability. Fig. 2 (b) shows the ratios between the largest and second-largest singular values of the matrix \mathbf{W} for the IEEE 14-bus system with different thresholds of the voltage stability. The results show that there is one large singular value and the other singular values are so small that they can be ignored compared to the largest singular value. This indicates that the rank of the matrix \mathbf{W} can be approximately considered to be 1. Fig. 3 (a) shows the singular values of the matrix \mathbf{W} for the IEEE 30-bus system with different thresholds of the voltage stability, and Fig. 3 (b) shows the ratios between the largest and second-largest singular values of the matrix \mathbf{W} for the IEEE 30-bus system with different thresholds of the voltage stability. The results have the similar patterns as those for the IEEE 14-bus system. For the IEEE 57-bus system and the IEEE 118-bus system, the ratios between the largest and second-largest singular values of the matrix \mathbf{W} are 7.23×10^5 and 5.46×10^5 , respectively.

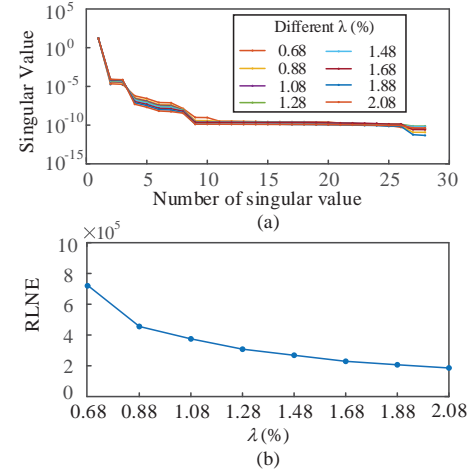


Fig. 2. (a) Singular values of the matrix \mathbf{W} for IEEE 14-bus system. (b) Ratio between the largest and second-largest singular values of the \mathbf{W} matrix for IEEE 14-bus system.

B. Influences of Voltage Stability on OPF

1) *Influences on generation:* Fig. 4 (a), (b), and (c) show the generation costs with different voltage stability critical indices for IEEE 14-bus system, IEEE 30-bus system, and IEEE 57-bus system, respectively. The x-axis denotes λ representing the percentage of increase in the value of the voltage stability critical index σ_c with respect to σ_1 , and σ_1 is obtained based on the scenario without the voltage stability constraint. The values of σ_1 for IEEE 14-bus system, IEEE 30-bus system, and IEEE 57-bus system are 0.4986, 0.2349, and 0.1863, respectively. The y-axis denotes the generation costs.

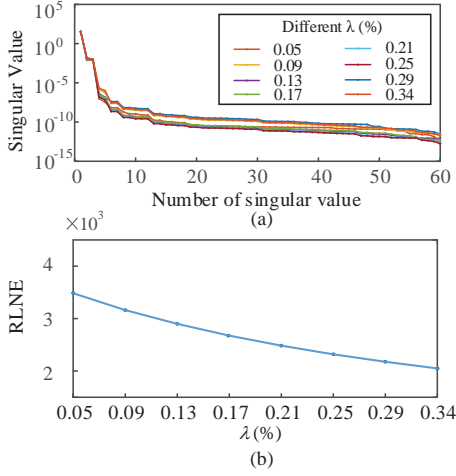


Fig. 3. (a) Singular values of the matrix \mathbf{W} for IEEE 30-bus system. (b) Ratio between the largest and second-largest singular values of the \mathbf{W} matrix for IEEE 30-bus system.

From the results, it is observed that a larger voltage stability critical index results in a higher generation cost. However, the differences of the generation costs under different voltage stability critical indices are not large. This indicates that the voltage stability constraint has a small impact on real power of generators. Fig. 5 (a) and (b) show reactive power differences between the scenario with the voltage stability constraint and the scenario without the voltage stability constraint under different values of σ_c . The colorbar on the right side of the figure represents λ . The x-axis denotes the generators, and the y-axis represents the power differences. For IEEE 30-bus system, when the percentage of increase in the values of SMV is 30.6%, the reactive power of G_2 decreases by 12.593 compared to the case without the voltage stability constraint. When the percentage of increase in the values of SMV is 8.6%, the reactive power of G_2 decreases by 2.714 compared to the case without the voltage stability constraint. We tested the cases with a large increase in the voltage stability critical index since this test is to show the influences of increasing voltage stability critical indices on real/reactive power generation. Because the rank-one constraint of the matrix \mathbf{W} is relaxed in the proposed model, it is possible that the accuracy of the results of some cases may decrease. However, the overall trend of the influences of increasing voltage stability critical indices on real/reactive power generation can be obtained. From the results, it is observed that a large reactive power output difference will be caused by a change of the voltage stability critical index.

We also have performed tests for systems under heavy load conditions. Fig. 6 (a) shows the singular values of the matrix \mathbf{W} for the IEEE 30-bus system with 1.8 times load under different thresholds of the voltage stability, and Fig. 6 (b) shows the ratios between the largest and second-largest singular values of the matrix \mathbf{W} . Fig. 7 (a) shows the singular values of the matrix \mathbf{W} for the IEEE 57-bus system with 1.7 times load under different thresholds of the voltage stability, and Fig. 7 (b) shows the ratios between the largest and second-largest singular values of the matrix \mathbf{W} . From the results, we can find that the largest singular value of \mathbf{W} is much larger than the other singular values of \mathbf{W} . This indicates that the rank of \mathbf{W} can be approximately considered to be 1.

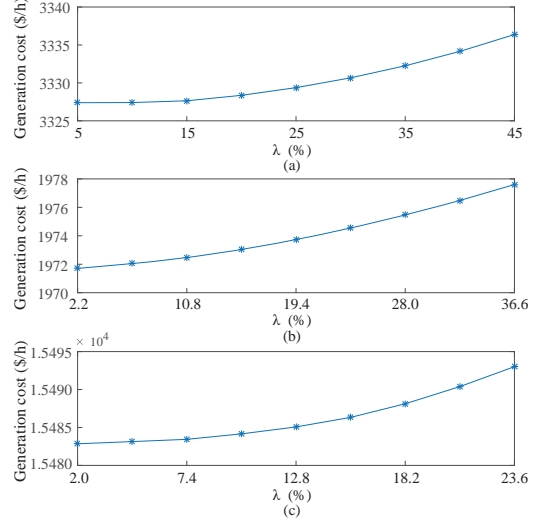


Fig. 4. Generation cost with different voltage stability critical indices for IEEE 30-bus system (a) and IEEE 57-bus system, respectively.

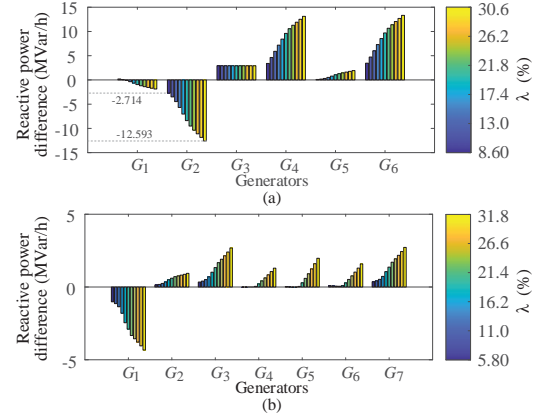


Fig. 5. (a) Reactive power difference with different voltage stability critical indices for IEEE 30-bus system (a) and IEEE 57-bus system (b), respectively.

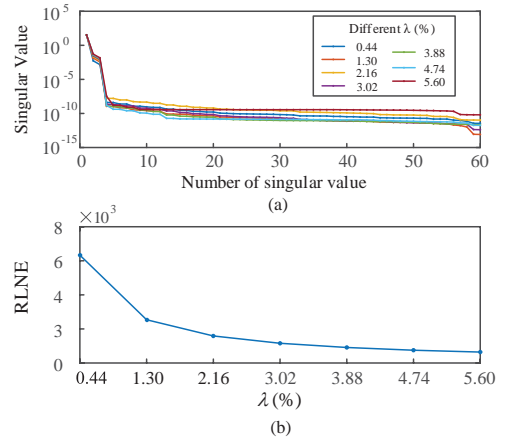


Fig. 6. (a) Singular values of the matrix \mathbf{W} for IEEE 30-bus system with 1.8 times load. (b) Ratio between the largest and second-largest singular values of the \mathbf{W} matrix for IEEE 30-bus system.

2) *PV bus influences*: In practical systems, the voltage magnitudes of generator buses are often regulated at certain

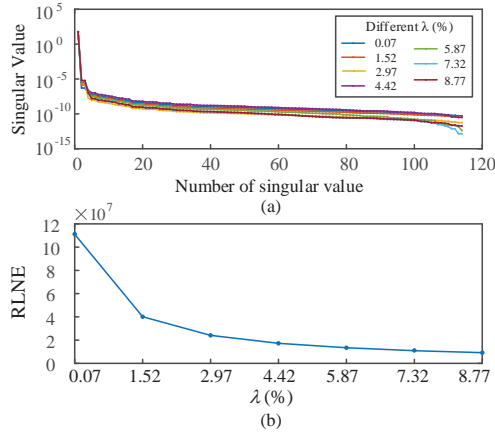


Fig. 7. (a) Singular values of the matrix \mathbf{W} for IEEE 57-bus system with 1.7 times load. (b) Ratio between the largest and second-largest singular values of the \mathbf{W} matrix for IEEE 57-bus system.

values. Table V shows the minimum singular value of Jacobian with different PV bus scenarios. For a system with more PV buses, the minimum singular value of the power flow Jacobian is much larger. Take the IEEE 14-bus system as an example, the minimum singular value with the bus 2 as a PV bus is 0.5922, the minimum singular value with the buses 2 and 3 as PV buses is 0.6099, and the minimum singular value with the buses 2, 3 and 6 as PV buses is 0.7033. When there are no PV buses in the system, the minimum singular value is 0.4986. In this simulation, the voltage magnitudes of PV buses are set to be 1.1. Table VI shows the real and reactive power of PV buses with different PV buses scenarios. When a bus connected to a generator works as a PV bus, the corresponding generator's reactive power has a large difference. The main reason for this is that much reactive power is needed to support the voltage magnitude at the PV buses.

Fig. 8 shows generation costs with different σ_c for the IEEE 14-bus system under different PV buses scenarios. For each scenario, when the voltage stability constraint works and the σ_c increases gradually, the generation cost has a higher value. Take the scenario 7 as an example, when $\sigma_c > 0.7033$, the generation cost increases gradually, and when $\sigma_c \leq 0.7033$, the generation cost remains the same as that for OPF without the voltage stability constraint.

TABLE V
MINIMUM SINGULAR VALUE OF JACOBIAN WITH DIFFERENT PV BUSES

Scenario No.	PV Bus	Minimum singular value of Jacobian
1	2	0.5922
2	3	0.5074
3	6	0.5647
4	2, 3	0.6099
5	2, 6	0.6804
6	3, 6	0.5853
7	2, 3, 6	0.7033

3) *Computational efficiency*: Table VII shows the average CPU time and iterations with the proposed voltage stability-constrained optimal power flow for different test systems. With a larger scale system, it takes a long CPU time to converge. However, we wish to emphasize that the scalability of the SDP formulation proposed in the paper can be greatly improved by

TABLE VI
REAL AND REACTIVE POWER WITH PV BUS SCENARIOS

Scenario No.	Buses	Generators	Real Power (p.u.)	Reactive Power (p.u.)
1	2	G_2	0.6190	0.9371
2	3	G_3	0.7486	0.5937
3	6	G_4	0.6137	0.4965
4	2	G_2	0.6232	0.7411
	3	G_3	0.7716	0.5006
5	2	G_2	0.6455	0.9351
	6	G_4	0.6262	0.7446
6	3	G_3	0.7477	0.5713
	6	G_4	0.6101	0.4974
	2	G_2	0.6516	0.7133
7	3	G_3	0.7901	0.5027
	6	G_4	0.6259	0.7830

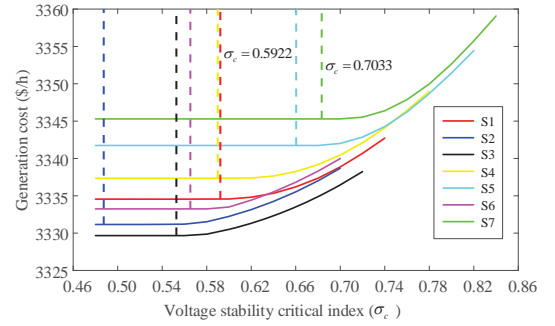


Fig. 8. Generation costs with different voltage critical indices under different PV bus scenarios, S1 - S7 denote the scenario 1 - the scenario 7 in Table V.

exploiting sparsity of the underlying power networks. Recent advances along the direction [48]–[51] can be easily tuned for the current formulation and is a subject of ongoing work. The main purpose of the current paper is to propose a convex optimization framework incorporating minimum singular value constraints in OPF problems, and the sparsity-exploitation is not included. Fig. 9 shows the duality gap with iterations for IEEE 14-bus, 30-bus, 57-bus and 118-bus systems. The algorithm converges between 35 and 40 iterations. The duality gaps are between 10^{-5} and 10^{-3} when the algorithm converges.

TABLE VII
CPU TIME AND ITERATIONS

Test systems	CPU time (s)	Iterations
IEEE 14-bus	3.02	34
IEEE 30-bus	10.54	39
IEEE 57-bus	120.12	43
IEEE 118-bus	2218.26	45

C. Discussion

The SDP-based VSC-OPF model should have the rank-one condition. Since the proposed model is relaxed by replacing the rank condition by the constraint $\mathbf{W} \succeq \mathbf{0}$, the resulting problem may have gaps. The future work can focus on the tightness of the relaxation [33], [34] and the rank constraint of the matrix \mathbf{W} by introducing the rank penalty functions [52]–[54] and some new hybrid constraints [55].

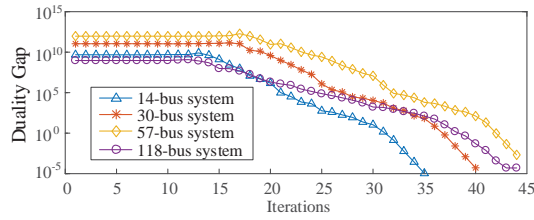


Fig. 9. Duality gaps with iterations for IEEE 14-bus, 30-bus, 57-bus, 118-bus systems.

With the increasing integration of resources with uncertainty, e.g., renewables and electric vehicles, these random variations have great impacts on system operations when considering voltage stability. The influences of renewable/load fluctuations can be represented as stochastic variables that are integrated to the proposed model in this paper, and the model will be extended to a stochastic programming model, with an expected function as the objective. The sample average approximation (SAA) method [56] can be used to approximate the expected objective of the stochastic problem by means of a sample average estimate derived from random samples. The resulting sample average approximating model is a deterministic model, which can be solved by the SDP technique.

V. CONCLUSIONS AND FUTURE WORK

To ensure reliable and secure operation in power system economic dispatch problems, we have proposed a VSC-OPF formulation using SDP relaxation of the conventional AC-OPF and LMI reformulation of the voltage stability constraint. To quantify the voltage stability margin, the minimum singular value of the power flow Jacobian has been used as a voltage stability index, which is incorporated into the conventional OPF model. To reformulate voltage stability constraint as a convex one, a positive semidefinite auxiliary matrix based on the power flow Jacobian has been constructed. The minimum singular value constraint on the power flow Jacobian is then effectively transformed to a LMI constraint on the minimum eigenvalue of the auxiliary matrix. We note that the reformulation of the voltage stability constraint is exact. The resulting SDP-based VSC-OPF model has been formulated and solved using the toolbox YALMIP and SDPT3. IEEE 14-bus, 30-bus, 57-bus, and 118-bus systems have been used to validate the proposed model. Simulation results show that the new VSC-OPF formulation effectively constrains the voltage stability margins and the effects on generation costs and generator outputs by imposing different margin constraints are presented.

REFERENCES

- [1] P. Kundur, J. Paserba, V. Ajjarapu, G. Andersson, A. Bose, C. Canizares, N. Hatziaargyriou, D. Hill, A. Stankovic, C. Taylor, T. V. Cutsem, and V. Vittal, "Definition and classification of power system stability IEEE/CIGRE joint task force on stability terms and definitions," *IEEE Trans. Power Syst.*, vol. 19, no. 3, pp. 1387–1401, Aug. 2004.
- [2] M. Milligan, B. Frew, E. Zhou, and D. J. Arent, "Advancing system flexibility for high penetration renewable integration," National Renewable Energy Laboratory Report, Oct. 2015. [Online]. Available: <http://www.nrel.gov/docs/fy16osti/64864.pdf>
- [3] H. D. Chiang and H. Sheng, "Available delivery capability of general distribution networks with renewables: Formulations and solutions," *IEEE Trans. Power Del.*, vol. 30, no. 2, pp. 898–905, Apr. 2015.
- [4] M. Todescato, J. W. Simpson-Porco, F. Dörfler, R. Carli, and F. Bullo, "Online distributed voltage stress minimization by optimal feedback reactive power control," *IEEE Trans. Control of Network Systems*, 2017, in press.
- [5] V. A. Venikov, V. A. Stroeve, V. I. Idelchick, and V. I. Tarasov, "Estimation of electrical power system steady-state stability in load flow calculations," *IEEE Trans. Power App. Syst.*, vol. 94, no. 3, pp. 1034–1041, May 1975.
- [6] A. Tiranuchit and R. J. Thomas, "A posturing strategy against voltage instabilities in electric power systems," *IEEE Trans. Power Syst.*, vol. 3, no. 1, pp. 87–93, Feb. 1988.
- [7] A. Tiranuchit, L. M. Ewerbring, R. A. Duryea, R. J. Thomas, and F. T. Luk, "Towards a computationally feasible on-line voltage instability index," *IEEE Trans. Power Syst.*, vol. 3, no. 2, pp. 669–675, May 1988.
- [8] P. A. Lof, T. Smed, G. Andersson, and D. J. Hill, "Fast calculation of a voltage stability index," *IEEE Trans. Power Syst.*, vol. 7, no. 1, pp. 54–64, Feb. 1992.
- [9] P. A. Lof, G. Andersson, and D. J. Hill, "Voltage stability indices for stressed power systems," *IEEE Trans. Power Syst.*, vol. 8, no. 1, pp. 326–335, Feb. 1993.
- [10] A. Berizzi, P. Finazzi, D. Dosi, P. Marannino, and S. Corsi, "First and second order methods for voltage collapse assessment and security enhancement," *IEEE Trans. Power Syst.*, vol. 13, no. 2, pp. 543–551, May 1998.
- [11] P. Kessel and H. Glavitsch, "Estimating the voltage stability of a power system," *IEEE Trans. Power Del.*, vol. 1, no. 3, pp. 346–354, July 1986.
- [12] B. Gao, G. K. Morison, and P. Kundur, "Voltage stability evaluation using modal analysis," *IEEE Trans. Power Syst.*, vol. 7, no. 4, pp. 1529–1542, Nov. 1992.
- [13] C. A. Canizares, F. L. Alvarado, C. L. DeMarco, I. Dobson, and W. F. Long, "Point of collapse methods applied to AC/DC power systems," *IEEE Trans. Power Syst.*, vol. 7, no. 2, pp. 673–683, May 1992.
- [14] I. Smon, G. Verbic, and F. Gubina, "Local voltage-stability index using Tellegen's theorem," *IEEE Trans. Power Syst.*, vol. 21, no. 3, pp. 1267–1275, Aug. 2006.
- [15] S. Corsi and G. N. Taranto, "A real-time voltage instability identification algorithm based on local phasor measurements," *IEEE Trans. Power Syst.*, vol. 23, no. 3, pp. 1271–1279, Aug. 2008.
- [16] G. Verbic and F. Gubina, "A new concept of voltage-collapse protection based on local phasors," *IEEE Trans. Power Del.*, vol. 19, no. 2, pp. 576–581, Apr. 2004.
- [17] Z. Wang, B. Cui, and J. Wang, "A necessary condition for power flow insolvability in power distribution systems with distributed generators," *IEEE Trans. Power Syst.*, vol. 32, no. 2, pp. 1440–1450, Mar. 2017.
- [18] C. Wang, B. Cui, and Z. Wang, "Analysis of solvability boundary for droop-controlled microgrids," *IEEE Trans. power syst.*, 2018, in press.
- [19] Y. Mansour, W. Xu, F. Alvarado, and C. Rinzin, "SVC placement using critical modes of voltage instability," *IEEE Trans. Power Syst.*, vol. 9, no. 2, pp. 757–763, May 1994.
- [20] H. Song, B. Lee, S.-H. Kwon, and V. Ajjarapu, "Reactive reserve-based contingency constrained optimal power flow (RCCOPF) for enhancement of voltage stability margins," *IEEE Trans. Power Syst.*, vol. 18, no. 4, pp. 1538–1546, Nov. 2003.
- [21] E. Vaahedi, Y. Mansour, C. Fuchs, S. Granville, M. D. L. Latore, and H. Hamadanizadeh, "Dynamic security constrained optimal power flow/Var planning," *IEEE Trans. Power Syst.*, vol. 16, no. 1, pp. 38–43, Feb. 2001.
- [22] M. De and S. K. Goswami, "Optimal reactive power procurement with voltage stability consideration in deregulated power system," *IEEE Trans. Power Syst.*, vol. 29, no. 5, pp. 2078–2086, Sep. 2014.
- [23] V. Ajjarapu, P. L. Lau, and S. Battula, "An optimal reactive power planning strategy against voltage collapse," *IEEE Trans. Power Syst.*, vol. 9, no. 2, pp. 906–917, May 1994.
- [24] B. Kermanshahi, K. Takahashi, and Y. Zhou, "Optimal operation and allocation of reactive power resource considering static voltage stability," in *International Conference on Power System Technology*, Aug. 1998, pp. 1473–1477.
- [25] T. Zabaoui, L. A. Dessaint, and I. Kamwa, "Preventive control approach for voltage stability improvement using voltage stability constrained optimal power flow based on static line voltage stability indices," *IET Generation, Transmission Distribution*, vol. 8, no. 5, pp. 924–934, May 2014.
- [26] B. Cui and X. A. Sun, "A new voltage stability-constrained optimal power flow model: Sufficient condition, socp representation, and relaxation," *IEEE Trans. Power Syst.*, vol. PP, no. 99, pp. 1–1, 2018.
- [27] Y. L. Chen, "Weak bus oriented reactive power planning for system security," *IEE Proceedings - Generation, Transmission and Distribution*, vol. 143, no. 6, pp. 541–545, Nov. 1996.
- [28] S. K. M. Kodsi and C. A. Canizares, "Application of a stability-constrained optimal power flow to tuning of oscillation controls in competitive electricity markets," *IEEE Trans. Power Syst.*, vol. 22, no. 4, pp. 1944–1954, Nov. 2007.
- [29] C. Canizares, W. Rosehart, A. Berizzi, and C. Bovo, "Comparison of voltage security constrained optimal power flow techniques," in *IEEE Power Engineering Society Meeting*, vol. 3, Jul. 2001, pp. 1680–1685.
- [30] R. J. Avalos, C. A. Canizares, and M. F. Anjos, "A practical voltage-stability-constrained optimal power flow," in *IEEE Power and Energy Society General Meeting*, July 2008, pp. 1–6.

- [31] L. Vandenberghe and S. Boyd, "Semidefinite programming," *SIAM Review*, vol. 38, no. 51, pp. 49–95, Mar. 1996.
- [32] S. Boyd and L. Vandenberghe, *Convex Optimization*. Cambridge University Press, 2009.
- [33] J. Lavaei and S. H. Low, "Zero duality gap in optimal power flow problem," *IEEE Trans. Power Syst.*, vol. 27, no. 1, pp. 92–107, Feb. 2012.
- [34] S. Sojoudi and J. Lavaei, "Physics of power networks makes hard optimization problems easy to solve," in *IEEE Power and Energy Society General Meeting*, July 2012, pp. 1–8.
- [35] B. Zhang and D. Tse, "Geometry of feasible injection region of power networks," in *49th Annual Allerton Conference on Communication, Control, and Computing (Allerton)*, Sep. 2011, pp. 1508–1515.
- [36] S. Bose, D. F. Gayme, S. Low, and K. M. Chandy, "Optimal power flow over tree networks," in *49th Annual Allerton Conference on Communication, Control, and Computing (Allerton)*, Sep. 2011, pp. 1342–1348.
- [37] S. Bose, D. F. Gayme, K. M. Chandy, and S. H. Low, "Quadratically constrained quadratic programs on acyclic graphs with application to power flow," *IEEE Trans. Control of Network Systems*, vol. 2, no. 3, pp. 278–287, Sep. 2015.
- [38] J. Lavaei, D. Tse, and B. Zhang, "Geometry of power flows and optimization in distribution networks," *IEEE Trans. Power Syst.*, vol. 29, no. 2, pp. 572–583, Mar. 2014.
- [39] S. Moghadas and S. Kamalasadan, "An architecture for voltage stability constrained optimal power flow using convex semi-definite programming," in *2015 North American Power Symposium (NAPS)*, Oct. 2015, pp. 1–6.
- [40] A. S. Pedersen, M. Blanke, and H. Jóhannsson, "Convex relaxation of power dispatch for voltage stability improvement," in *2015 IEEE Conference on Control Applications (CCA)*, Sept. 2015, pp. 1528–1533.
- [41] I. Dobson, "The irrelevance of load dynamics for the loading margin to voltage collapse and its sensitivities," in *Bulk Power Syst. Phenomena III: Voltage Stability Security Contr.*, Aug. 1994, pp. 509–519.
- [42] P. Sauer and M. Pai, "Power system steady-state stability and the load-flow jacobian," *IEEE Trans. power syst.*, vol. 5, no. 4, pp. 1374–1383, 1990.
- [43] T. Van Cutsem and C. Vournas, *Voltage Stability of Electric Power Systems*, ser. Power Electronics and Power Systems. Springer US, 2007. [Online]. Available: <https://books.google.com/books?id=ihbnBwAAQBAJ>
- [44] R. D. Zimmerman, C. E. Murillo-Sanchez, and R. J. Thomas, "Matpower: Steady-state operations, planning, and analysis tools for power systems research and education," *IEEE Trans. Power Syst.*, vol. 26, no. 1, pp. 12–19, Feb. 2011.
- [45] J. Lofberg, "YALMIP: a toolbox for modeling and optimization in matlab," in *IEEE International Conference on Robotics and Automation*, Sep. 2004, pp. 284–289.
- [46] K. C. Toh, M. Todd, and R. H. Tutuncu, "SDPT3 – a MATLAB software package for semidefinite programming," *Optimization Methods and Software*, vol. 11, pp. 545–581, 1999.
- [47] Simulation Data. [Online]. Available: <http://icseg.iti.illinois.edu/power-cases/>
- [48] D. K. Molzahn, J. T. Holzer, B. C. Lesieutre, and C. L. DeMarco, "Implementation of a large-scale optimal power flow solver based on semidefinite programming," *IEEE Trans. Power Syst.*, vol. 28, no. 4, pp. 3987–3998, Nov. 2013.
- [49] R. A. Jabr, "Exploiting sparsity in SDP relaxations of the OPF problem," *IEEE Trans. Power Syst.*, vol. 27, no. 2, pp. 1138–1139, May 2012.
- [50] M. Fukuda, M. Kojima, K. Murota, and K. Nakata, "Exploiting sparsity in semidefinite programming via matrix completion I: General framework," *SIAM J. Optim.*, vol. 11, no. 3, pp. 647–674, 2011.
- [51] K. Nakata, K. Fujisawa, M. Fukuda, M. Kojima, and K. Murota, "Exploiting sparsity in semidefinite programming via matrix completion II: implementation and numerical results," *Mathematical Programming*, vol. 95, no. 2, pp. 303–327, 2003.
- [52] R. Madani, S. Sojoudi, and J. Lavaei, "Convex relaxation for optimal power flow problem: Mesh networks," *IEEE Trans. Power Syst.*, vol. 30, no. 1, pp. 199–211, Jan. 2015.
- [53] D. K. Molzahn, C. Jozs, I. A. Hiskens, and P. Panciatici, "A laplacian-based approach for finding near globally optimal solutions to opf problems," *IEEE Trans. Power Syst.*, vol. 32, no. 1, pp. 305–315, Jan. 2017.
- [54] R. Madani, M. Ashraphijuo, and J. Lavaei, "Promises of conic relaxation for contingency-constrained optimal power flow problem," *IEEE Trans. Power Syst.*, vol. 31, no. 2, pp. 1297–1307, Mar. 2016.
- [55] C. Coffrin, H. L. Hijazi, and P. V. Hentenryck, "Strengthening the sdp relaxation of ac power flows with convex envelopes, bound tightening, and valid inequalities," *IEEE Trans. Power Syst.*, vol. 32, no. 5, pp. 3549–3558, Sep. 2017.
- [56] A. J. Kleywegt, A. Shapiro, and T. H. de Mello, "The sample average approximation method for stochastic discrete optimization," *SIAM Journal on Optimization*, vol. 12, no. 2, pp. 479–502, 2002.



Chong Wang (M'16) received the B.E and M.S degrees in electrical engineering from Hohai University, Nanjing, China, in 2009 and 2012, and the Ph.D. degree in electrical engineering from The University of Hong Kong, Hong Kong, in 2016. He was a postdoctoral researcher at The University of Hong Kong in 2016, and was a postdoctoral researcher at Iowa State University from 2017 to 2018. He is currently an Associate Professor with the College of Energy and Electrical Engineering, Hohai University, Nanjing, China.

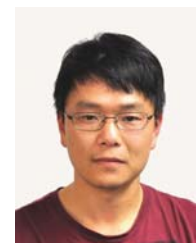
His research interests include optimization and its applications in power systems, smart grids, integration of renewable energy sources, and cyber-physical systems.



Cui Bai (S'15) is a postdoctoral appointee at Argonne National Laboratory. He received the B.S. degrees in Electrical Engineering and Computer Engineering from Shanghai Jiao Tong University, Shanghai, China and the University of Michigan, Ann Arbor, MI, respectively, in 2011. He received the M.S. and Ph.D. degrees in Electrical and Computer Engineering from the Georgia Institute of Technology, Atlanta, GA, in 2014 and 2018, respectively. His research interests include power system stability and power system optimization.



Zhaoyu Wang (S'13-M'15) is the Harpole-Pentair Assistant Professor with Iowa State University. He received the B.S. and M.S. degrees in electrical engineering from Shanghai Jiaotong University in 2009 and 2012, respectively, and the M.S. and Ph.D. degrees in electrical and computer engineering from Georgia Institute of Technology in 2012 and 2015, respectively. He was a Research Aid at Argonne National Laboratory in 2013 and an Electrical Engineer Intern at Corning Inc. in 2014. His research interests include power distribution systems, microgrids, renewable integration, power system resilience, and power system modeling. He is the Principal Investigator for a multitude of projects focused on these topics and funded by the National Science Foundation, the Department of Energy, National Laboratories, PSERC, Iowa Energy Center, and Industry. Dr. Wang received the IEEE PES General Meeting Best Paper Award in 2017 and the IEEE Industrial Application Society Prize Paper Award in 2016. Dr. Wang is the Secretary of IEEE Power and Energy Society Award Subcommittee. He is an editor of IEEE Transactions on Smart Grid and IEEE PES Letters.



Chenghong Gu (M'14) was born in Anhui province, China. He received the Bachelor's degree from the Shanghai University of Electric Power, Shanghai, China, in 2003, and the Master's degree from the Shanghai Jiao Tong University, Shanghai, China, in 2007, both in electrical engineering. He received the Ph.D. degree from the University of Bath, U.K. He is currently a Lecturer with the Department of Electronic and Electrical Engineering, University of Bath. His major research interest is in multi-vector energy system, smart grid, and power economics..